CT angiography with 15 mL contrast material injection on time-resolved imaging for endovascular abdominal aortic aneurysm repair

Horinouchi, Hiroki ; Sofue, Keitaro ; Nishii, Tatsuya ; Maruyama, Koji ; Sasaki, Koji ; Gentsu, Tomoyuki ; Ueshima, Eisuke ; Okada, Takuya ;…

(Citation)
European Journal of Radiology,126:108861

(Issue Date)
2020-05

(Resource Type)
journal article

(Version)
Accepted Manuscript

(URL)
https://hdl.handle.net/20.500.14094/90007092

CT angiography with 15 mL contrast material injection on time-resolved imaging for endovascular abdominal aortic aneurysm repair

Hiroki Horinouchi, MD[1,2]; Keitaro Sofue, MD, PhD[1,3]; Tatsuya Nishii, MD, PhD[1,2]; Koji Maruyama, MD, PhD [1]; Koji Sasaki, MD[1]; Tomoyuki Gentsu, MD, PhD [1,3]; Eisuke Ueshima, MD, PhD[1]; Takuya Okada, MD, PhD[1]; Masato Yamaguchi, MD, PhD[1]; Koji Sugimoto, MD, PhD[1,3]; Takamichi Murakami, MD, PhD[1]

[1] Department of Radiology, Kobe University Graduate School of Medicine, Kobe, Japan

[2] Department of Radiology, National Cerebral and Cardiovascular Center, Suita, Japan

[3] Center for Endovascular Center, Kobe University Hospital, Kobe, Japan

Address all correspondence to:

Keitaro Sofue, MD, PhD

Assistant professor of Radiology, Kobe University Graduate School of Medicine

7-5-2, Kusunoki-cho, Chuo-ku, Kobe, 650-0017, Japan

Phone: +81 (78) 382-6104

Fax: +81 (78) 382-6129

E-mail: keitarosofue@gmail.com

CT angiography with 15 mL contrast material injection on time-resolved imaging for endovascular abdominal aortic aneurysm repair

- Original article -

Abstract

Purpose: To assess the utility of whole-aorta CT angiography (CTA) with 15 mL contrast material (CM) on time-resolved imaging for endovascular abdominal aortic repair (EVAR).

Methods: Twenty-six patients with a high-risk of post-contrast acute kidney injury (PC-AKI) underwent CTA with 15 mL CM using temporal maximum intensity projection (tMIP-CTA) generated from time-resolved imaging. The aortoiliac CT values were measured. Two observers measured the arterial diameters in unenhanced CT and tMIP-CTA images, and image quality was evaluated on a 5-point scale. The presence of the accessory renal artery, inferior mesenteric artery (IMA) occlusion, and instructions for use (IFU) of EVAR were evaluated.

Results: CT examinations were successfully performed, and no patients developed PC-AKI. The mean CT values of the whole aorta were 267.5 ± 51.4 HU, which gradually decreased according to the distal levels of the aorta. Bland-Altman analysis revealed excellent agreement for the external arterial diameter measurements between unenhanced CT and tMIP-CTA. Excellent interobserver agreement was achieved for the measurements of the external (ICCs, 0.910−0.992) and internal arterial diameters (ICCs, 0.895−0.993). Excellent or good overall image quality was achieved in 24 (92%) patients. The presence of the accessory renal artery, IMA occlusion and the assessment of IFU were in 100% agreement. Multivariate analysis revealed aortic volume as the most significant independent factor associated with strong aortic enhancement (p= 0.004).

Conclusions: Whole-aorta tMIP-CTA on time-resolved imaging is useful for maintaining contrast enhancement and image quality for EVAR planning, and can substantially reduce the amount of CM.

Abbreviations:

CTA	Computed tomography angiography
CM	Contrast materials
EVAR	Endovascular abdominal aortic repair
AAA	Abdominal aortic aneurysm
PC-AKI	Post-contrast acute kidney injury
tMIP	Temporal maximum intensity projection
IMA	Inferior mesenteric artery
IFU	Instructions for use
eGFR	Estimated glomerular filtration rate
sCr	Serum creatinine
TTP	Time to peak
CNR	Contrast to noise ratio
ICC	Intraclass correlation coefficient

1. Introduction

Endovascular abdominal aortic repair (EVAR) has become an alternative to conventional open repair for the treatment of abdominal aortic aneurysm (AAA) due to shorter patient hospital stays and lower perioperative mortality [1, 2]. Accurate assessment of the whole aorta using preoperative imaging examination is mandatory to evaluate the morphologic criteria for EVAR and the risk of complications [3].

Computed tomography angiography (CTA) is currently the standard preoperative imaging for EVAR [3, 4]. The advantages of CTA include high spatial resolution with a short examination time, allowing high quality, multiplanar reformatted, and three-dimensional reconstructed images. However, whole-aortic CTA requires a large amount of contrast material (CM) to obtain appropriate vascular attenuation with wide scan coverage. On the other hand, impaired renal function has been associated with negative outcomes and increased mortality rates after EVAR [5]. The most important risk factor for post-contrast acute kidney injury (PC-AKI) is impaired renal function [6]. For EVAR planning, the total amount of CM needs to be minimized to prevent PC-AKI in high-risk patients.

Time-resolved CTA has been a technique for the evaluation of flow dynamics in the brain, extremities, and endoleaks after EVAR [7-9]. Until recently, time-resolved CTA could not cover the whole aorta due to the limited z-axis coverage. Adaptive 4D Spiral Plus (Siemens Healthcare, Forchheim, Germany) has enabled the acquirement volume perfusion data with a wide z-axis coverage, which can potentially visualize the whole aorta in separate phases of single scan mode.

Additionally, temporal maximum intensity projection (tMIP) equipped with a commercial software package (*Syngo.* CT Dynamic Angio) is an image-based post-processing technique to provide three-dimensional (3D) volume images by summing the maximum CT values of multiphasic data [7, 10]. Thus, we hypothesized that Adaptive 4D Spiral mode in combination with tMIP can provide CTA throughout the whole aorta with a substantial reduction of CM.

The purpose of this study was to assess the utility of whole-aorta CTA with 15 mL CM on time-resolved imaging for EVAR of AAA.

2. Materials and methods

2.1. Patient population

This study was a retrospective analysis and approved by the institutional review board with waiver of written informed consent. Between June 2016 and January 2018, 26 patients (mean age, 78.8 years; age range, 65–95 years; 22 males and 4 females; mean body weight 58.8 ± 12.2 kg; weight range 33.6−78.1 kg) who planned to undergo EVAR for infrarenal AAA and had high risk of PC-AKI were selected. PC-AKI was defined as an increase in serum creatinine (sCr) of ≥ 0.3mg/dl, or of ≥ 1.5-1.9 times baseline in the 48-72 hours following CM administration. High risk of PC-AKI was also defined as having risk factors including impaired renal function of estimated glomerular filtration rates (eGFR) <45 mL/min/1.73m2 or multiple risk factors [6, 11]. Eighteen patients had impaired renal function with eGFR <45 mL/min/1.73m^2. The remaining eight patients had multiple risk factors for PC-AKI, including eGFR <60 mL/min/1.73m^2, hypertension, hyperuricemia, diabetes mellitus, and proteinuria. The patients' characteristics, including body mass index, sCr, eGFR, ejection fraction, and cardiac output, are summarized in Table 1.

2.2. CT examination protocol

All CT examinations were performed with a third-generation dual-source CT scanner (SOMATOM Force; Siemens Healthcare). Firstly, unenhanced breath-hold CT of the chest and abdomen, referred to as "conventional unenhanced CT" (120-kVp; detector configuration, 0.6 × 192

mm; rotation time, 0.25 sec.; section thickness, 5.0-mm; reconstruction interval, 5.0-mm; reconstruction kernel, Br40) was obtained to localize the whole-aortic route. Time-resolved CTA was then obtained using a shuttle mode for bidirectional (cranio-caudal and caudo-cranial) table movement with continuous image acquisition over a scan range of 63 cm. The scan parameters were as follows; 0.6 × 192 mm section acquisition with the z-flying focal spot, 0.25 sec. per rotation, variable pitch factor, and 70-kVp tube voltage. Automatic tube current selection (CARE Dose 4D) was used to minimize the radiation dose. A total of ten spiral phases were acquired every 2.5 sec. for the first five phases and 5.0 sec. for the following five phases. Thus, the overall acquisition time was 35.35 sec.

Intravenous injection of CM was performed through a 20-gauge catheter placed in the right antecubital vein using an automated dual power injector (Nemoto Kyorindo; Tokyo, Japan). Test bolus measured the time to peak (TTP) by using region of interest (ROI) placement at the level of the ascending aorta. A 10 mL (1 mL CM diluted with 9 mL saline) test bolus followed by 20 mL saline flush at a rate of 3 mL/sec. was conducted. Scan start delay was set two seconds before the TTP measured by test bolus. The main bolus administration consisted of 15 mL CM followed by 40 mL saline flush at an injection rate of 3 mL/sec. Individual CM concentrations were selected according to each patient's body weight to set the individual iodine load around 75 mgI/kg: >70 kg; 370 mgI/mL (Iopromide; Fuji Pharma, Tokyo, Japan) , 55–70 kg; 300 mgI/mL (Iopamiron; Bayer Pharma, Osaka, Japan), <55 kg; 240 mgI/mL (Omnipaque; Daiichi Sankyo, Tokyo, Japan). Radiation

doses were measured on conventional unenhanced CT and time-resolved CTA. Volume CT dose index ($CTDI_{vol}$) and dose-length product (DLP) presented by the CT equipment were also taken.

2.3. Postprocessing and image reconstruction

All images were reconstructed with a 1.0-mm slice thickness, with the use of a medium smooth soft tissue kernel (Bv36) and advanced modeled iterative reconstruction (ADMIRE) strength level of 4. All ten phases of reconstructed image data from time-resolved CTA were transferred to workstation (*Syngo.*via; Siemens Healthcare), and tMIP-CTA images were created using a commercial software package (*Syngo.* CT Dynamic Angio; Siemens Healthcare). This software primarily aims to visualize vessel enhancement from dynamic CT datasets with the help of automatic motion correction, noise reduction, and non-rigid registration, and can be used to obtain information on blood flow from the arterial to the late phase (Fig. 1). The original time-resolved CTA images from ten phases dynamic CT datasets are also available (Supplemental Digital Content 1, which demonstrates MIP images from time-resolved CTA in ten phases). Meanwhile, we utilized this software to create whole-aorta CTA by summing a total of ten phase images.

The steps taken to create the whole-aorta CTA is summarized in Figure 1. Firstly, the transferred images were forwarded to motion correction with Alion Myocard mode and adapted using 4D Noise Reduction. Next, the Volume Creation tool was activated. The tMIP images were then produced to visualize the highest pixel value of the images in all ten phases. Finally, the tMIP

image data was reconstructed in the axial plane with 1.0-mm thickness and 1.0-mm interval, where after three-dimensional reconstructions consisting of standard MIP and volume-rendering reconstructions were created (Fig. 2). Aortic volume was calculated using a manually segmented volume-rendering image of the entire aorta. This image data was transferred to a dedicated PACS workstation.

2.4. Quantitative image analysis

Quantitative image quality was assessed on reconstructed 1.0-mm thick axial images of the tMIP-CTA by a board-certified radiologist ([*blinded for review*] with 9-years' experience). Intravascular CT values (in HU) of the arteries were measured according to mean CT values in circular region of interests (ROIs) at six locations: the ascending and descending aorta at pulmonary trunk level, pararenal aorta, AAA, and bilateral common iliac artery (Fig. 3). The ROIs were placed as broadly as possible by using a circular ROI in the lumen of arteries, avoiding the vascular wall, calcifications, plaque, and artifacts. We introduced mean CT values and standard deviation (SD) throughout the whole aorta, which were intended to represent how highly and homogeneously aortic enhancement was achieved in tMIP-CTA. Contrast to noise ratio (CNR) at each level was also calculated using the following equation:

CNR = (HU of vessel - HU of psoas muscle) / SD of psoas muscle.

Additionally, two independent board-certified radiologists ([*blinded for review*] and [*blinded for review*] with 8- and 9-years' experience) manually measured the diameters of the arteries. Maximum transverse external artery diameter was measured on conventional unenhanced CT and tMIP-CTA images to examine the differences. Maximum transverse internal artery diameter was measured on tMIP-CTA images to examine interobserver agreement. Seven locations were measured on each image as follows: the ascending and descending aorta at pulmonary trunk level, pararenal aorta, AAA, terminal aorta, right and left common iliac artery (Fig. 3).

2.5. Qualitative image analysis

Qualitative image analyses were performed by the two radiologists ([*blinded for review*] and [*blinded for review*]). Each observer reviewed tMIP-CTA images and graded overall image quality, aortic contrast enhancement, aortic marginal blurring, visualization of the proximal (1st–2nd branch) and distal (renal hilum–intrarenal branch) renal artery, and 3D reconstructed image quality on a 5-point Likert scale (1= unacceptable; 2= poor; 3= fair; 4= good; 5= excellent). In addition, the presence of the accessory renal artery and inferior mesenteric artery (IMA) occlusion were evaluated. Concordance between the two observers regarding the technical suitability for EVAR was evaluated. Both observers independently evaluated whether each case could be within or outside instructions for use (IFU). Outside IFU was defined as not fulfilling the following points for the evaluation of IFU:

1) proximal neck length > 10mm, angulation < 60 degrees, and diameter between 19 mm and 32mm, 2) iliac sealing-zone diameter between 8 mm and 25 mm, and length > 15 mm (Fig. 4).

2.6. Statistical analysis

Continuous variables were presented as mean ± standard deviations and range. Categorical variables were presented as absolute numbers and percentages. Wilcoxon signed-rank test was used for the comparison of radiation exposure between tMIP-CTA and conventional unenhanced CT and for the comparison of sCr levels between before and after CT examination. For each imaging analysis, intraclass correlation coefficients (ICCs) were calculated to evaluate interobserver agreement as follows: >0.80, excellent; 0.6−0.80, good; 0.40−0.60, moderate; 0.20−0.40, fair; and <0.20, poor. Bland-Altman analysis was performed to show the distribution of differences of the aortic diameters between in conventional unenhanced CT and tMIP-CTA images. Agreement between the observers regarding the presence of the accessory renal artery, the presence of IMA occlusion, and the assessment of IFU were calculated as percentages.

A multivariate linear regression analysis was performed to determine the clinical factors associated with strong (mean CT value throughout the whole aorta) and homogeneous (mean SD throughout the whole aorta) aortic contrast enhancement. The coefficient of determination (R^2) was calculated to indicate how well data fitted the statistical model.

Statistical analyses were performed using a statistical software (SPSS for Windows, version 20; IBM, Chicago, Il), and a p-value < 0.05 was considered statistically significant.

3. Results

All CT examinations were successfully performed without complications and technical failure. Mean iodine dose, mean iodine delivery rate, and mean iodine load were 76.7 ± 10.3 mgI/kg, 0.88 ± 0.15 g/s, and 4.4 ± 0.74 g, respectively. Mean $CTDI_{vol}$ and DLP were significantly higher in tMIP-CTA (16.9 ± 4.0 mGy and 1030.4 ± 251.3 mGy × cm) than those in conventional unenhanced CT (9.1 ± 1.7 mGy and 656.2 ± 143.8 mGy × cm) ($p< 0.001$) (Table 1). In 25 patients whose blood samples could be taken within seven days after CT examination (mean, 2.4 days; range 1−6 days), the mean sCr levels before and after CTA were 1.53 ± 0.95 mg/dL and 1.46 ± 0.92 mg/dL ($p= 0.97$), and no patients developed PC-AKI (Fig. 5).

3.1. Quantitative image analysis

The mean CT values and SD of the whole aorta was 267.5 ± 51.4 HU. The mean CT value was greater than 200 HU in 25 (96%) patients and greater than 250 HU in 21 (81%) patients at all levels of the aorta. The CT values and CNR gradually decreased according to the distal levels of the aorta (Fig. 6). For the measurements of the external aortic diameters, excellent interobserver agreements (ICCs, 0.910−0.992) were observed between conventional unenhanced CT and tMIP-CTA (Table 2). Bland-Altman analysis for external aortic diameter demonstrated excellent agreement and no systematic over or under estimation between conventional unenhanced CT and tMIP-CTA.

Interobserver agreements for the measurements of the internal aortic diameters were also excellent (ICCs, 0.895−0.993) (Table 3).

3.2. Qualitative image analysis

Qualitative image analysis scores were high, with good to excellent interobserver agreement in 24 (92%) patients (Table 4). Visualization of the distal renal artery was relatively inferior compared to the proximal renal artery. The presence of accessory renal artery and IMA occlusion were in 100% agreement between the two observers. Notably, 100% agreement was achieved regarding the assessment of anatomy within or outside IFU. Both observers evaluated eleven patients as outside IFU on tMIP-CTA.

3.3. Influence of high and homogeneous aortic enhancement in tMIP-CTA

Multivariate linear regression analyses showed that the aortic volume was the most significant independent factor associated with high aortic enhancement (p= 0.004), and sex was also significant (p= 0.02). No clinical factors had significant effect on homogeneous aortic enhancement (Table 5).

4. Discussion

The results of our study demonstrated that whole-aorta CTA using tMIP on time-resolved imaging achieved a substantial reduction of CM while maintaining sufficient aortic enhancement and image quality, and that none of the high-risk patients developed PC-AKI with excellent interobserver agreement for the quantitative and qualitative measurements. These findings indicate that whole-aorta tMIP-CTA with 15 mL CM on time-resolved imaging can provides accurate aortic morphologic characteristics for EVAR planning.

A third-generation dual-source CT scanner enabled us to acquire time-resolved imaging with a z-axis coverage of up to 80 cm. In this study, we attempted to acquire whole-aortic CTA with 15 mL CM by capturing the volume perfusion of CM using 70-kVp time-resolved imaging. Although aortic enhancement in each phase image on time-resolved imaging was heterogeneous, to evaluate precise vascular morphology, the sum of the maximum CT values in ten phase data using tMIP achieved homogeneous whole-aortic contrast enhancement. In order to maintain diagnostic quality, previous studies reported that minimal attenuation of the aorta ought to be greater than 200–250 HU [12, 13]. Our results showed sufficient contrast enhancement of the aorta, in which 96% and 81% of the patients achieved 200 HU and 250 HU mean attenuation of the whole aorta. Eventually, our technique achieved a substantial reduction of CM while maintaining sufficient aortic enhancement compared with other previously published techniques, including transarterial catheter-directed CTA rather than low-tube-voltage CTA [14-16]. On the other hand, the CT values gradually decreased

according to the distal level of the aorta. A possible explanation could be that CM stagnates within the aorta, which is supported by our analysis in which aortic volume influenced strong aortic contrast enhancement. The trapping of administered CM in dead space or aortic branches might also affect aortic contrast enhancement.

The tMIP-CTA consisted of a sum of ten phase images, and thus required automatic motion correction, noise reduction, and nonrigid registration. These post-processing techniques potentially affect accurate measurements of the arteries, because the aortic diameter changes significantly during the cardiac cycle with a mean increase of up to 10% [17, 18]. In contrast, our Bland-Altman analysis revealed small differences regarding the external diameter measurements between in conventional unenhanced CT and tMIP-CTA images. Our qualitative analysis demonstrated good to excellent image quality in 92% of the patients with less aortic marginal blurring and clear visualization of the proximal renal artery. Whole-aorta tMIP-CTA could maintain image quality even during longer acquisition times. By contrast, respiratory and peristaltic motions may cause remarkable changes in morphology and texture, which can result in a deterioration of image quality in tMIP-CTA images. This concern was raised by inferior qualitative image scores in visualization of the distal renal artery compared with the proximal renal artery in the present study. Therefore, it should be noted that tMIP-CTA cannot fully replace standard CTA examination.

Our findings have important clinical implications. First, tMIP-CTA did not impair renal function even in high-risk patients for PC-AKI. Second, tMIP-CTA provided required aortic

morphologic characteristics for EVAR planning. In our qualitative analysis, perfect agreement of the assessment of IFU with excellent agreement of arterial diameter measurements was accomplished between the two observers. Their evaluation of the accessory renal artery and IMA occlusion was also in 100% agreement. The assessment of IFU, accessory renal artery and IMA are essential for evaluating the risk of complications after EVAR. Hostile anatomy outside IFU was an independent risk factor of type I endoleak with a 3.8−15% incidence [3, 19]. Accessory renal artery coverage during EVAR induced segmental renal infarction [20]. Patent IMA was associated with the incidence of type II endoleak after EVAR [21]. Based on these findings, tMIP-CTA can allow for the accurate assessment for preoperative planning of EVAR and the risk assessment of complication after EVAR in high-risk patients for PC-AKI. Meanwhile, tMIP-CTA is limited in evaluating microvascular anatomy because of higher image noise and slight misregistration even with the use of the latest post-processing techniques. Additionally, tMIP-CTA images, which were derived from ten phase datasets, heightened radiation exposure even though a 70-kVp tube voltage with iterative reconstruction algorithm was used to minimize the radiation dose [4, 22]. Increasing radiation exposure is a trade-off for the substantial reduction of CM in patients with severe renal dysfunction, and radiation doses of tMIP-CTA would be acceptable with refer to diagnostic reference levels (DRLs) [23].

The present study has several limitations because of its single-institution, retrospective nature. This background made it difficult to precisely evaluate clinical outcomes. Our study lacked

standards of reference such as conventional CTA because patients had severe renal dysfunction. Although excellent inter-examination agreement for external arterial measurements between conventional unenhanced CT and tMIP-CTA would assure the quality of the tMIP-CTA images, further comparative studies are necessary. Secondly, the present study applied fixed amount of 15 mL CM at an injection rate of 3 mL/sec to simplify the CT examination protocol. Several factors for the optimization of the CT examination could not be validated, such as the amount of CM, number of acquisitions in time-resolved imaging, and iterative reconstruction strength level, which is needed for the further refinement of the examination [24]. Lastly, the patients in our study population were Asian and tended to be of a smaller habitus compared with Western populations, thus 70-kVp images may not be appropriate for larger patients, especially when using high pitch mode [25]. In high-weight patients, 70-kVp scans affect image quality due to increased image noise caused by radiation scattering and absorption effect. In Western populations, although a lower kVp setting would be appropriate, this yielded a relatively lower boost of contrast enhancement while maintaining lower image noise compared with 70-Vp setting [22, 24]. Although the superiority of the tMIP-CTA for the substantial reduction of CM is unaffected, the optimal kVp setting and amount of CM need to be examined.

In conclusion, whole-aorta tMIP-CTA on time-resolved imaging with 15 mL is useful method for maintaining aortic contrast enhancement and image quality for EVAR planning, and can substantially reduce the amount of CM.

References

[1] F.A. Lederle, J.A. Freischlag, T.C. Kyriakides, et al., Outcomes following endovascular vs open repair of abdominal aortic aneurysm: a randomized trial, JAMA 302 (2009) 1535-1542.

[2] R.M. Greenhalgh, L.C. Brown, J.T. Powell, et al., Endovascular versus open repair of abdominal aortic aneurysm, N. Engl. J. Med. 362 (2010) 1863-1871.

[3] A.C. Picel, N. Kansal, Essentials of endovascular abdominal aortic aneurysm repair imaging: preprocedural assessment, Am. J. Roentgenol. 203 (2014) 347-357.

[4] L. Faggioni, M. Gabelloni, Iodine Concentration and Optimization in Computed Tomography Angiography: Current Issues, Invest. Radiol. 51 (2016) 816-822.

[5] A. Saratzis, P. Sarafidis, N. Melas, et al., Impaired renal function is associated with mortality and morbidity after endovascular abdominal aortic aneurysm repair, J. Vasc. Surg. 58 (2013) 879-885.

[6] A.J. van der Molen, P. Reimer, I.A. Dekkers, et al., Post-contrast acute kidney injury - Part 1: Definition, clinical features, incidence, role of contrast medium and risk factors : Recommendations for updated ESUR Contrast Medium Safety Committee guidelines, Eur. Radiol. 28 (2018) 2845-2855.

[7] H.G. Kortman, E.J. Smit, M.T. Oei, et al., 4D-CTA in neurovascular disease: a review, Am. J. Neuroradiol. 36 (2015) 1026-1033.

[8] T. Henzler, N. Vogler, B. Lange, et al., Low dose time-resolved CT-angiography in pediatric

patients with venous malformations using 3rd generation dual-source CT: Initial experience, Eur. J. Radiol. Open 3 (2016) 216-222.

[9] W.H. Sommer, C.R. Becker, M. Haack, et al., Time-resolved CT angiography for the detection and classification of endoleaks, Radiology 263 (2012) 917-926.

[10] E.J. Smit, E.J. Vonken, I.C. van der Schaaf, et al., Timing-invariant reconstruction for deriving high-quality CT angiographic data from cerebral CT perfusion data, Radiology 263 (2012) 216-225.

[11] F. Stacul, A.J. van der Molen, P. Reimer, et al., Contrast induced nephropathy: updated ESUR Contrast Media Safety Committee guidelines, Eur. Radiol. 21 (2011) 2527-2541.

[12] Y. Nakayama, K. Awai, Y. Funama, et al., Lower tube voltage reduces contrast material and radiation doses on 16-MDCT aortography, Am. J. Roentgenol. 187 (2006) 490-497.

[13] K.T. Bae, Intravenous contrast medium administration and scan timing at CT: considerations and approaches, Radiology 256 (2010) 32-61.

[14] C.M. Chen, S.Y. Chu, M.Y. Hsu, et al., Low-tube-voltage (80 kVp) CT aortography using 320-row volume CT with adaptive iterative reconstruction: lower contrast medium and radiation dose, Eur. Radiol. 24 (2014) 460-468.

[15] P. Hou, X. Feng, J. Liu, et al., Iterative reconstruction in single-source dual-energy CT angiography: feasibility of low and ultra-low volume contrast medium protocols, Br. J. Radiol. 90 (2017) 20160506.

[16] A.J. Isaacson, L.M. Burke, R. Vallabhaneni, et al., Ultralow Iodine Dose Transarterial Catheter-Directed CT Angiography for Fenestrated Endovascular Aortic Repair Planning, Ann. Vasc. Surg. 35 (2016) 234-237.

[17] M. Prokop, H.O. Shin, A. Schanz, et al., Use of maximum intensity projections in CT angiography: a basic review, Radiographics 17 (1997) 433-451.

[18] R. Iezzi, C. Di Stasi, R. Dattesi, et al., Proximal aneurysmal neck: dynamic ECG-gated CT angiography--conformational pulsatile changes with possible consequences for endograft sizing, Radiology 260 (2011) 591-598.

[19] J. Oliveira-Pinto, N. Oliveira, F. Bastos-Goncalves, et al., Long-term results of outside "instructions for use" EVAR, J. Cardiovasc. Surg. 58 (2017) 252-260.

[20] M. Sadeghi-Azandaryani, H. Zimmermann, I. Korten, et al., Altered renal functions in patients with occlusion of an accessory renal artery after endovascular stenting of an infrarenal aneurysm, J. Vasc. Surg. 65 (2017) 635-642.

[21] T.J. Ward, S. Cohen, R.S. Patel, et al., Anatomic risk factors for type-2 endoleak following EVAR: a retrospective review of preoperative CT angiography in 326 patients, Cardiovasc Intervent. Radiol. 37 (2014) 324-328.

[22] A. Winklehner, R. Goetti, S. Baumueller, et al., Automated attenuation-based tube potential selection for thoracoabdominal computed tomography angiography: improved dose effectiveness, Invest. Radiol. 46 (2011) 767-773.

[23] K.M. Kanal, P.F. Butler, D. Sengupta, et al., U.S. Diagnostic Reference Levels and Achievable Doses for 10 Adult CT Examinations, Radiology 284 (2017) 120-133.

[24] M.M. Lell, G. Jost, J.G. Korporaal, et al., Optimizing contrast media injection protocols in state-of-the art computed tomographic angiography, Invest. Radiol. 50 (2015) 161-167.

[25] M. Lurz, M.M. Lell, W. Wuest, et al., Automated tube voltage selection in thoracoabdominal computed tomography at high pitch using a third-generation dual-source scanner: image quality and radiation dose performance, Invest. Radiol. 50 (2015) 352-360.

Figure legends

Figure 1. Image showing a step for the creation of whole-aortic CTA using temporal MIP generated from Time-resolved imaging.

All ten phases reconstructed image data from time-resolved CTA were forward to motion correction with Alion Myocard mode and segmented by using 4D Noise Reduction, and Volume Creation Tool was activated in the case navigator area (yellow square). The tMIP images were then produced to visualize the highest pixel value of the images in all ten phases in the mini toolbar located at the bottom of the tMIP image segment (red square).

Figure 2. Maximum intensity projection images from time-resolved imaging in four of ten time-points and summing of all ten phases.

Maximum intensity projection (MIP) images in 2nd (a), 4th (b), 5th (c), and 7th (d) spiral phase images on time-resolved imaging, and in summing a total of ten spiral phase images (e).

Figure 3. Whole-aorta volume-rendering images and measurement at different anatomic regions of the aorta.

Volume rendering images (a) and transverse CTA images at levels of ascending and descending aorta (b), pararenal aorta (c), abdominal aortic aneurism (d), terminal aorta (e), and right and left common iliac artery (f).

Figure 4. Instructions for use of EVAR stent-graft.

Following points were assessed for the evaluation of instruction for use: 1) proximal neck length, angulation, and diameter and 2) iliac sealing-zone diameter and length

Figure 5. Serum creatinine levels between before and after CTA.

Mean serum creatinine levels before and after CTA were 1.53 ± 0.95 mg/dL and 1.46 ± 0.92 mg/dL (P= 0.97). No patients developed post-contrast acute kidney injury after CTA.

Figure 6. Differences and distributions of CT value and contrast-to-noise ratio in different anatomic regions of the aorta.

The CT values and CNR gradually decreased according to the distal anatomic regions of the aorta. The mean CT values and SD of the whole aorta was 267.5 ± 51.4 HU.

Supplemental Digital Content 1. Wmv

Maximum intensity projection (MIP) CTA images can visualize anatomical and blood flow information from ten phase dynamic CT datasets.

Table 1. Patient Characteristics and Radiation Exposure.

Patient characteristics		
Age (years)	78.8 ± 5.9 (65−94)	
Sex		
Male	85% (22/26)	
Female	15% (4/26)	
Weight (kg)	58.8 ± 12.2 (33.6−78.1)	
Height (cm)	163.0 ± 6.7 (148.0−173.4)	
Body mass index (kg/m^2)	22.0 ± 3.8 (15.3−28.4)	
Serum creatinine (mg/dL)	1.51 ± 0.94 (0.63−2.47)	
eGFR ($mL/min/1.73m^2$)	41.1 ± 16.2 (8.7−90.5)	
Iodine load (mgI/kg)	76.7 ± 10.3 (63.3−107.1)	
Ejection faction (%)	62.0 ± 9.0 (32.1−79.9)	
Cardiac output (mL/s)	4.74 ± 1.35 (3.00−7.60)	
Aortic volume (mL)	565.2 ± 158.8 (333.7−1043.0)	
Radiation exposure	**Conventional unenhanced CT**	**Time-resolved CTA**
$CTDI_{vol}$ (mGy)	9.1 ± 1.7 (7.0–14.2)	16.9 ± 4.0 (9.3−23.2)
DLP (mGy.cm)	656.2 ± 143.8 (493.7–1123.5)	1030.4 ± 251.3 (559.9−1400.3)

Data are presented as mean ± standard deviation (ranges) for the continuous variables and proportion (counts) for the categorical variables.

eGFR= estimated glomerular filtration rate. $CTDI_{vol}$= volume CT dose index. DLP= dose-length product.

Table 2. Measurements of External Diameter of the Arteries, Interexamination and Interobserver Agreement both on Temporal MIP-CTA and Conventional Unenhanced CT images.

Variables	Observer 1			Observer 2			Interobserver agreement	
	External diameter (mm)		Bland-Altman analysis	External diameter (mm)		Bland-Altman analysis		
	tMIP-CTA	Conventional		tMIP-CTA	Conventional		tMIP-CTA	Conventional
Ascending aorta	42.3 ± 5.5 (32.1−55.3)	42.3 ± 5.1 (33.1−54.7)	0.00 (-0.33−0.34)	41.8 ± 5.4 (32.9−56.1)	42.0 ± 5.2 (33.0−55.4)	0.20 (-0.10−0.49)	0.982 (0.960−0.992)	0.986 (0.970−0.994)
Descending aorta	33.0 ± 2.8 (28.2−38.5)	32.6 ± 2.5 (28.1−37.3)	-0.40 (-0.82−0.02)	33.1 ± 3.1 (27.2−39.1)	32.9 ± 2.9 (28.6−39.3)	-0.12 (-0.36−0.13)	0.976 (0.946−0.989)	0.910 (0.810−0.959)
Pararenal aorta	25.2 ± 3.7 (19.7−34.4)	25.4 ± 3.4 (20.0−35.2)	0.21 (-0.06−0.48)	25.6 ± 3.7 (20.1−34.4)	25.3 ± 3.4 (20.4−34.9)	-0.24 (-1.02−0.55)	0.934 (0.853−0.970)	0.987 (0.970−0.994)
AAA	50.2 ± 7.2 (35.0−62.8)	49.9 ± 7.0 (34.4−62.4)	-0.34 (-0.92−0.24)	50.5 ± 7.2 (35.1−63.1)	50.5 ± 7.3 (35.0−62.9)	0.06 (-0.15−0.27)	0.991 (0.981−0.995)	0.977 (0.949−0.989)
Terminal aorta	27.1 ± 7.0 (17.3−43.4)	26.7 ± 6.9 (17.7−42.7)	-0.33 (-1.16−0.51)	26.8 ± 6.7 (18.2−42.9)	27.0 ± 6.8 (18.3−42.8)	0.13 (-0.01−0.27)	0.961 (0.914−0.982)	0.991 (0.981−0.996)
Right CIA	17.5 ± 3.3 (12.9−26.1)	17.3 ± 3.3 (13.3−26.6)	-0.20 (-0.44−0.03)	17.4 ± 3.0 (13.4−24.5)	17.7 ± 3.5 (13.7−26.8)	0.32 (-0.04−0.69)	0.958 (0.908−0.981)	0.978 (0.952−0.990)
Left CIA	17.2 ± 4.2 (10.5−29.2)	17.0 ± 3.7 (11.4−28.4)	-0.19 (-0.56−0.18)	17.2 ± 4.0 (10.9−29.0)	17.1 ± 3.8 (11.8−28.4)	-0.09 (-0.38−0.20)	0.992 (0.983−0.997)	0.980 (0.957−0.991)

Measurement data are presented as mean ± standard deviations. Numbers in parentheses are ranges.

Statistical data in parenthesis are presented as 95% limits agreement for Bland-Altman analysis and 95% confidence interval for ICCs, respectively.

tMIP= temporal maximum intensity projection. Conventional= conventional unenhanced CT. AAA= abdominal aortic aneurysm. CIA= common iliac artery.

Table 3. Measurements of Internal Diameter of the Arteries on Temporal MIP-CTA.

Variables	Observer 1	Observer 2	Interobserver agreement
Ascending aorta	38.1 ± 5.5 (27.8–49.8)	38.6 ± 5.4 (28.2–51.2)	0.993 (0.984−0.997)
Descending aorta	28.1 ± 3.1 (21.1–37.2)	28.9 ± 2.7 (24.0–36.1)	0.924 (0.838−0.965)
Pararenal aorta	21.1 ± 3.5 (15.3–30.7)	21.9 ± 3.7 (16.0–32.6)	0.969 (0.931−0.986)
AAA	36.0 ± 10.0 (18.3–58.5)	36.2 ± 10.2 (19.0–60.0)	0.895 (0.831−0.948)
Terminal aorta	19.4 ± 4.9 (13.3–32.6)	20.0 ± 4.8 (13.8–31.2)	0.988 (0.973−0.994)
Right CIA	14.2 ± 3.4 (8.0–22.2)	14.9 ± 3.4 (8.3–22.8)	0.971 (0.937−0.987)
Left CIA	13.3 ± 3.4 (7.0–19.9)	14.1 ± 3.5 (7.7–20.8)	0.975 (0.946−0.989)

Measurement data are presented as mean ± standard deviation in millimeters. Numbers in parentheses are ranges.

Statistical data in parenthesis are presented as 95% confidence interval for ICCs.

AAA= abdominal aortic aneurysm. CIA= common iliac artery.

Table 4. Qualitative Image Analyses on Temporal MIP-CTA Images.

Variables	Observer 1	Observer 2	Interobserver agreement
Overall image quality	4.4 ± 0.6 (3–5)	4.6 ± 0.5 (4–5)	0.678 (0.282–0.856)
Contrast enhancement	4.5 ± 0.7 (3–5)	4.4 ± 0.6 (3–5)	0.642 (0.202–0.840)
Aortic marginal blurring	4.3 ± 0.6 (3–5)	4.3 ± 0.5 (4–5)	0.654 (0.443–0.821)
Visualization of the proximal renal artery	5.0 ± 0.2 (4–5)	4.9 ± 0.3 (4–5)	0.846 (0.643–0.949)
Visualization of the distal renal artery	4.2 ± 0.8 (3–5)	3.8 ± 0.8 (3–5)	0.746 (0.433–0.886)
3D reconstructed image quality	4.5 ± 0.6 (3–5)	4.6 ± 0.5 (4–5)	0.692 (0.481–0.849)
Presence of accessory renal artery	50% (13/26)	50% (13/26)	100% (26/26)
Presence of inferior mesenteric artery occlusion	31% (8/26)	31% (8/26)	100% (26/26)
Assessment of anatomy outside instructions for use	42% (11/26)	42% (11/26)	100% (26/26)

Data are presented as mean ± standard deviation (range) for Numbers in parentheses are ranges.

Table 5. Multivariate Linear Regression Models for Factors Associated with Insufficient and Heterogeneous Aortic Enhancement in Temporal MIP-CTA.

Variables	Coefficient	Standard error	β	t value	p-value
Insufficient enhancement					
Age	1.54 (-2.48–5.56)	1.70	0.25	0.90	0.40
Sex	63.74 (14.72–112.77)	20.73	0.79	3.07	0.02
Weight	-5.46 (-18.56–7.65)	5.54	-1.97	-0.98	0.36
Height	5.48 (-3.69–14.66)	3.88	1.13	1.41	0.20
Body mass index	16.25 (-18.66–51.15)	14.76	1.87	1.10	0.31
Creatinine	-14.70 (-37.41–8.01)	9.60	-0.47	-1.53	0.17
eGFR	-0.18 (-1.43–1.07)	0.53	-0.10	-0.34	0.74
Iodine load	-0.48 (-2.66–1.70)	0.92	-0.15	-0.52	0.62
Ejection fraction	-0.88 (-2.60–0.84)	0.73	-0.28	-1.21	0.26
Cardiac output	3.67 (-7.99–15.33)	4.93	0.15	0.74	0.48
Aortic volume	-0.21 (-0.32–-0.09)	0.05	-0.77	-4.24	0.004
Heterogeneous enhancement					
Age	2.53 (-0.19–5.24)	1.15	1.05	2.20	0.06
Sex	22.15 (-10.93–55.24)	13.99	0.69	1.58	0.16
Weight	2.99 (-5.85–11.84)	3.74	2.71	0.80	0.45
Height	-2.10 (-8.29–4.10)	2.62	-1.09	-0.80	0.45
Body mass index	-5.93 (-29.49–17.62)	9.96	-1.71	-0.59	0.57
Creatinine	10.08 (-5.25–25.40)	6.48	0.82	1.55	0.16
eGFR	0.42 (-0.42–1.27)	0.36	0.59	1.19	0.27
Iodine load	-0.25 (-1.72–1.22)	0.62	-0.20	-0.39	0.70
Ejection fraction	0.35 (-0.81–1.51)	0.49	0.28	0.72	0.49
Cardiac output	-2.89 (-10.76–4.98)	3.33	-0.29	-0.87	0.41
Aortic volume	-0.02 (-0.09–0.06)	0.03	-0.14	-0.45	0.67

Note. − Numbers in parentheses are 95% confidence intervals.

Coefficient of determination and analysis of variance were: Insufficient enhancement (R^2= 0.577, P< 0.001) and Heterogeneous enhancement (R^2= 0.271, P< 0.05).

β= standardized coefficient. eGFR= estimated glomerular filtration rate.

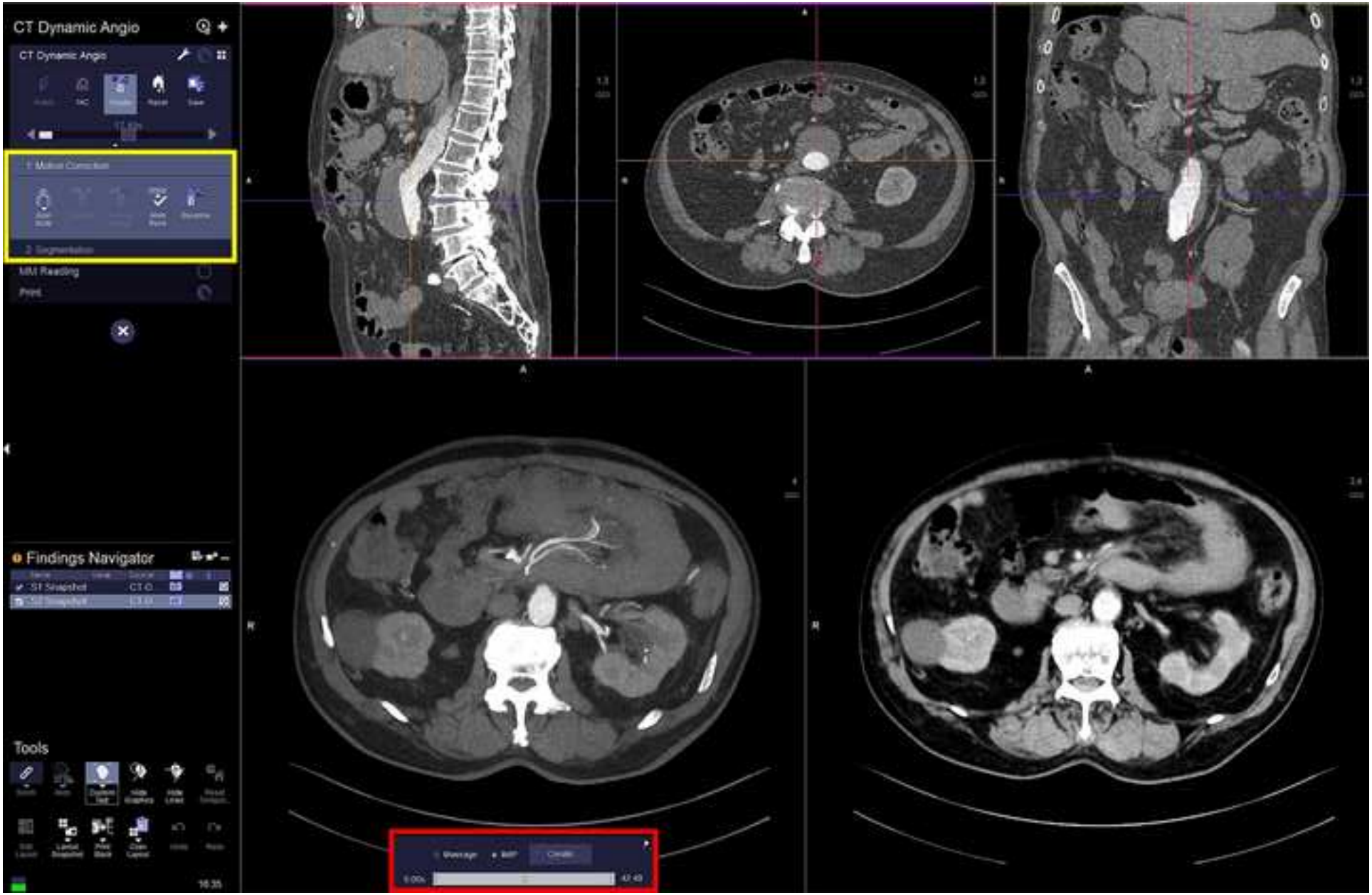
CT Dynamic Angio
CT Dynamic Angio
MM Reading
Print
Findings Navigator
Tools

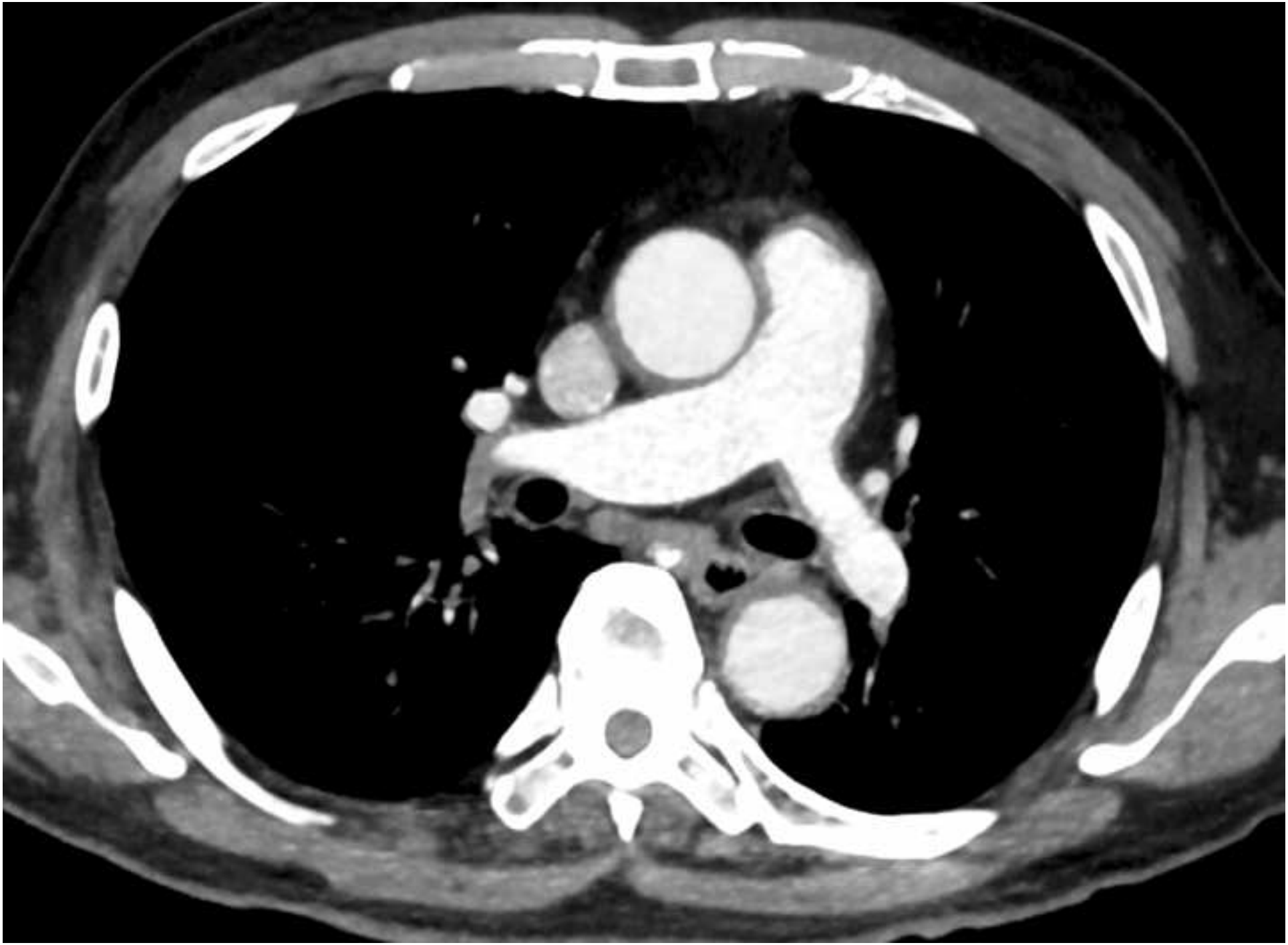

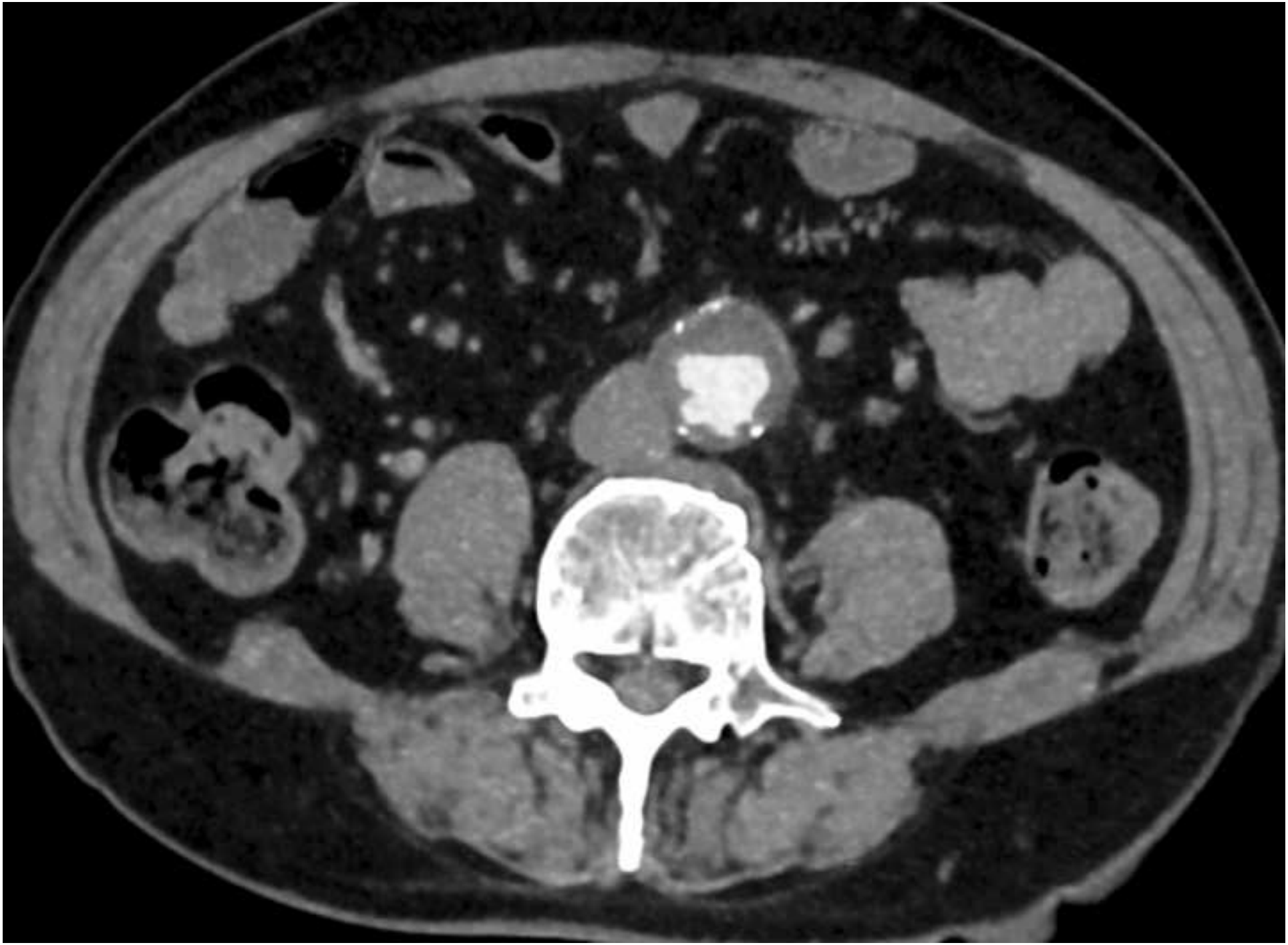

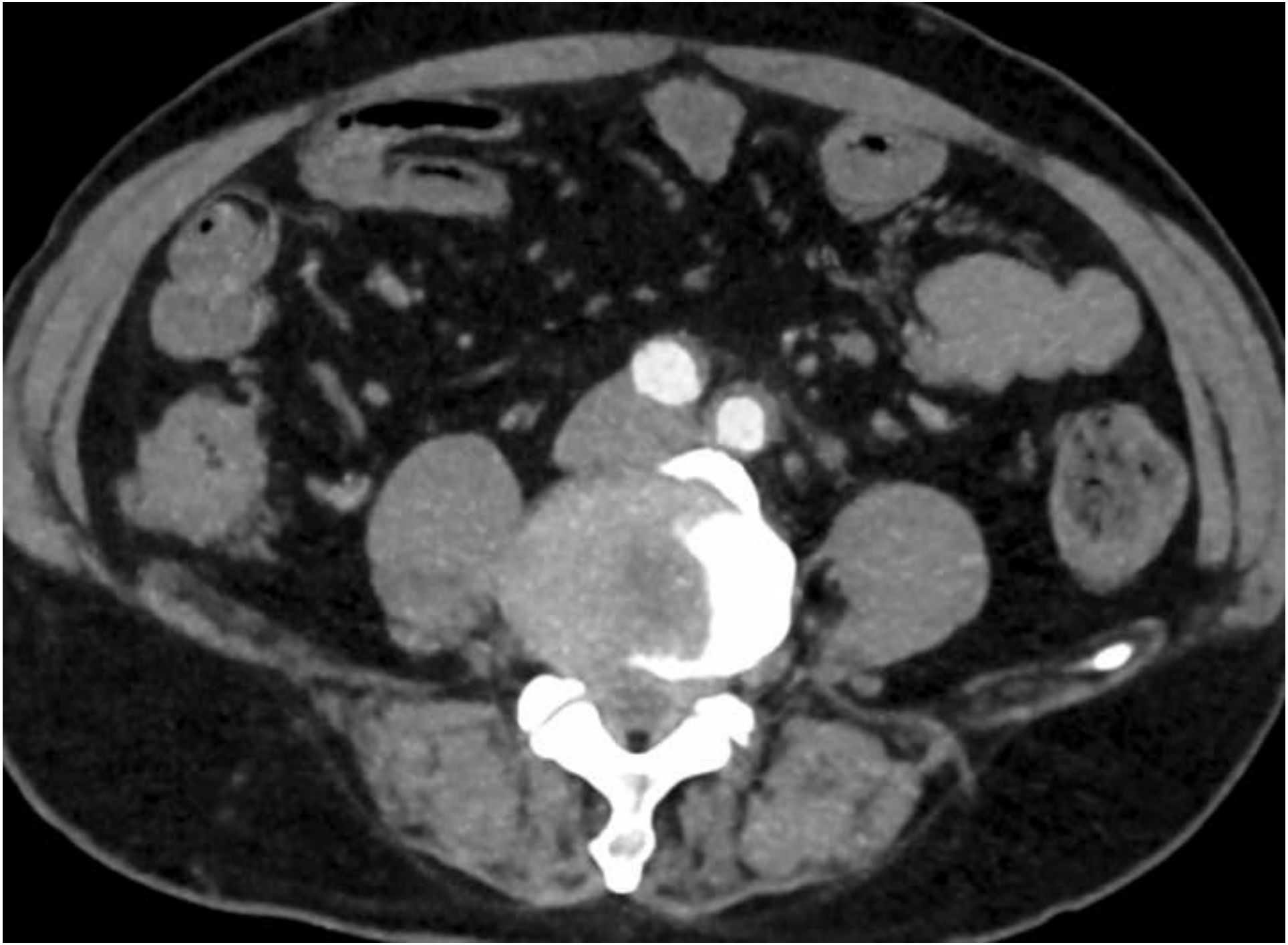

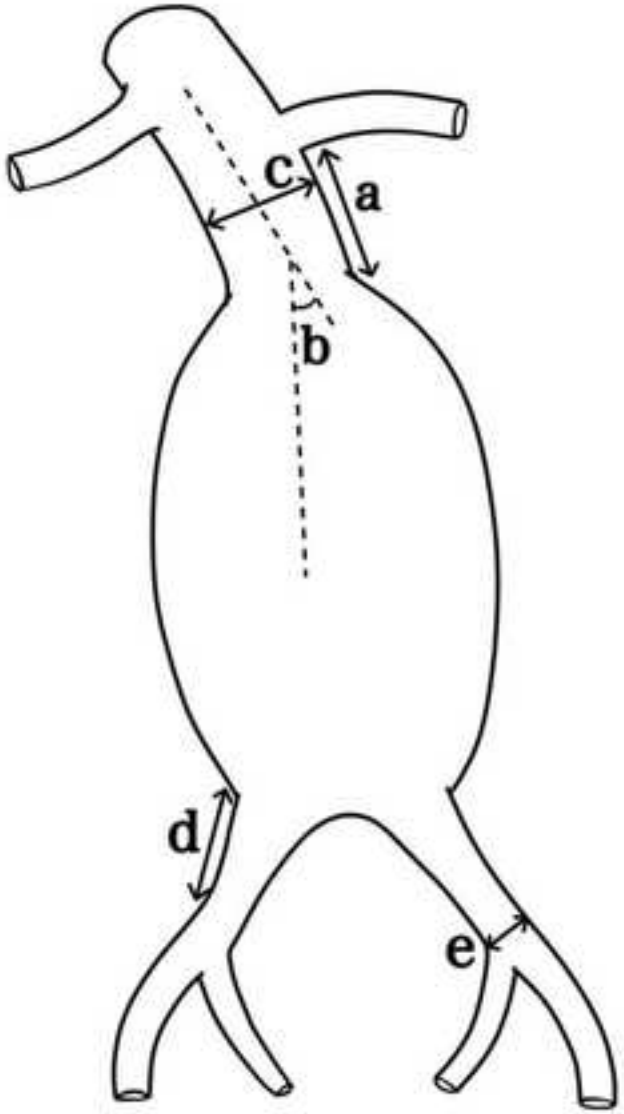

Evaluation of instruction for use (IFU) of stent-graft	
Proximal neck configuration	
a. Minimal length (mm)	10 mm
b. Maximal angulation (°)	60 °
c. Diameter (mm)	19–32 mm
Iliac arterial configuration	
d. Minimal length (mm)	15 mm
e. Diameter (mm)	8–25 mm

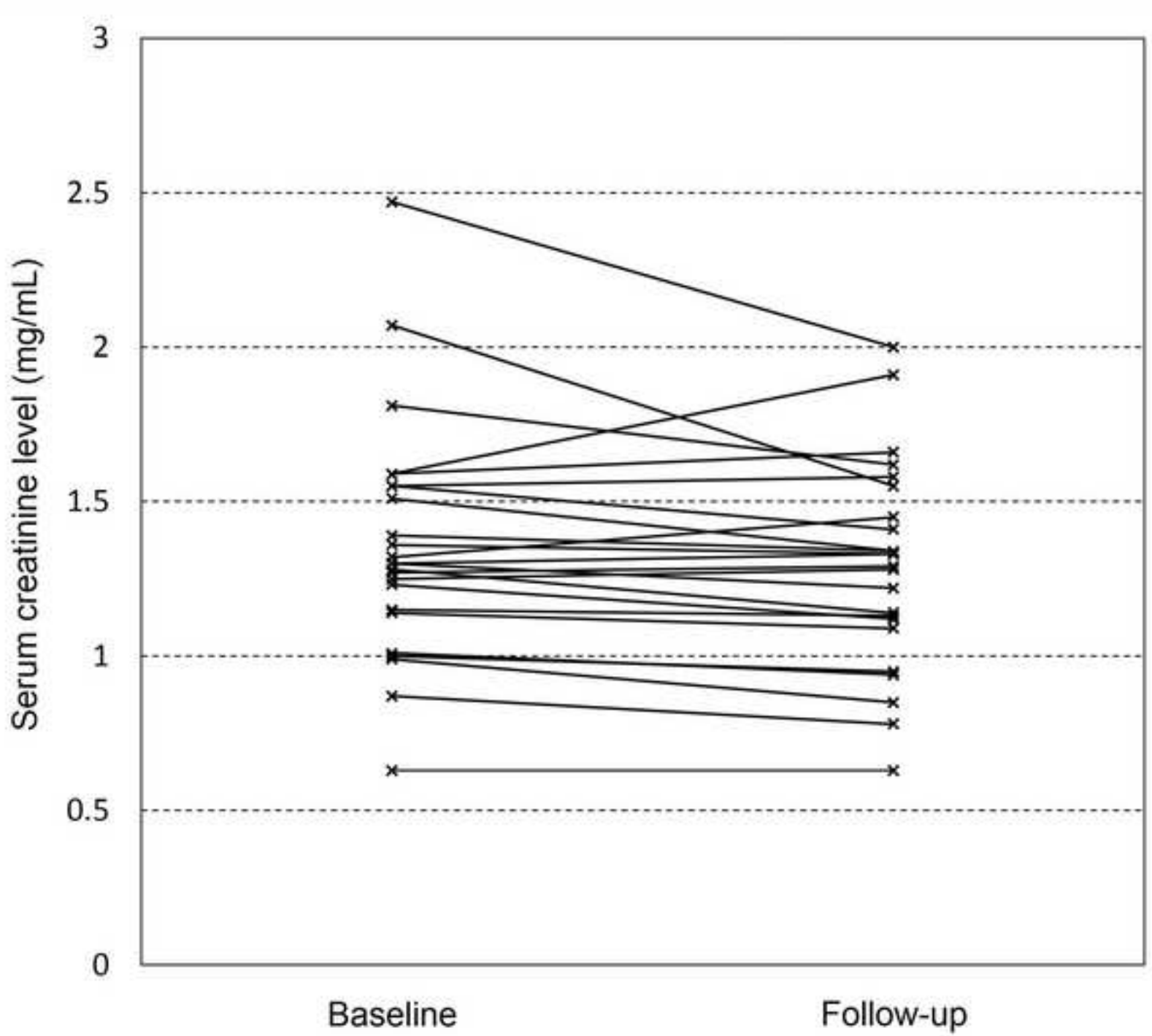
Serum creatinine level (mg/mL)
3
2.5
2
1.5
1
0.5
0
Baseline
Follow-up

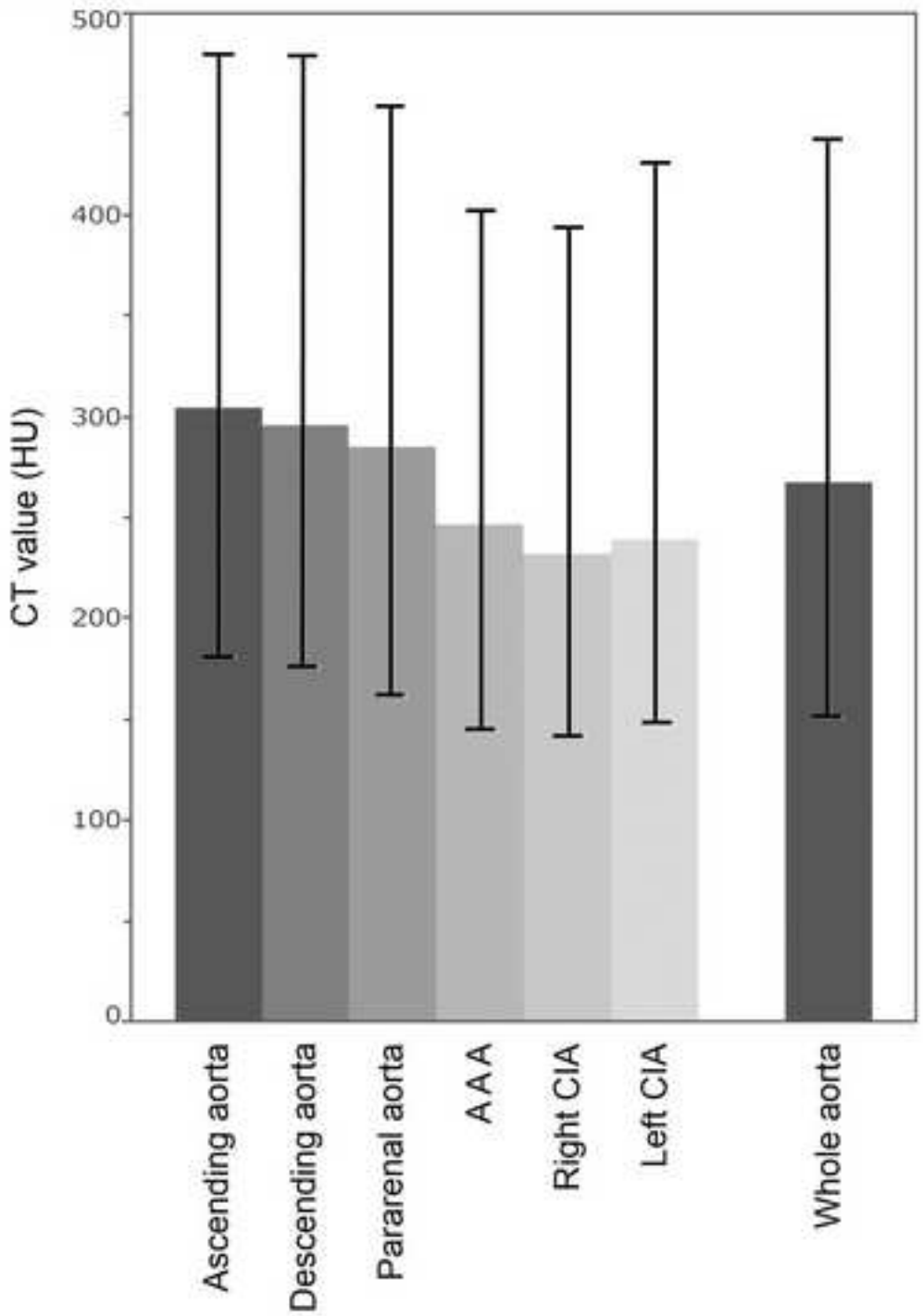
CT value (HU)
500
400
300
200
100
0
Ascending aorta
Descending aorta
Pararenal aorta
A A A
Right CIA
Left CIA
Whole aorta

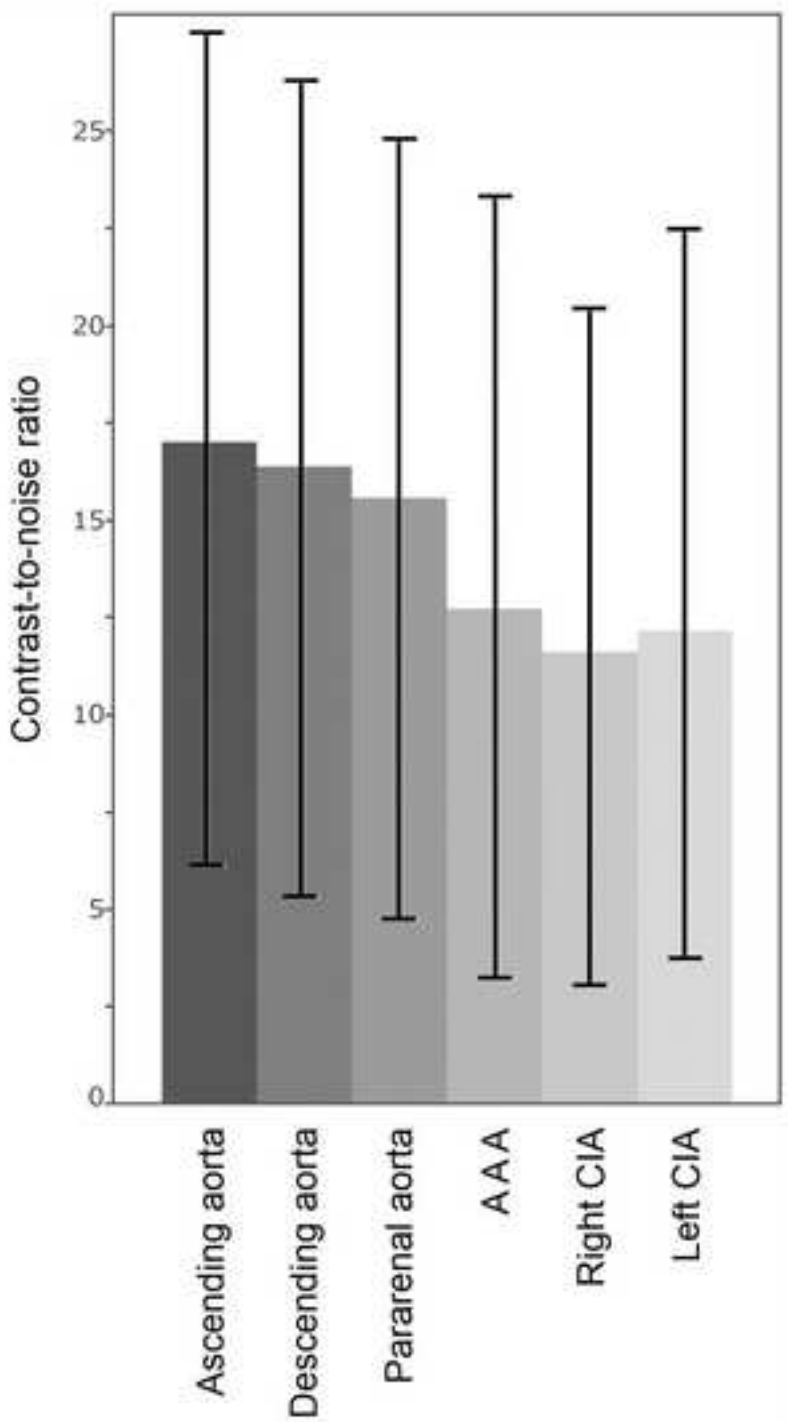
Contrast-to-noise ratio
25
20
15
10
5
0
Ascending aorta
Descending aorta
Pararenal aorta
A A A
Right CIA
Left CIA